Mineralogical Magazine, October 2012, Vol. 76(5), pp. 1153–1163

Raberite, $Tl_5Ag_4As_6SbS_{15}$, a new Tl-bearing sulfosalt from Lengenbach quarry, Binn valley, Switzerland: description and crystal structure

L. Bindi[1,2,*], F. Nestola[3], A. Guastoni[4], L. Peruzzo[5], M. Ecker[6] and R. Carampin[5]

[1] Dipartimento di Scienze della Terra, Università degli Studi di Firenze, Via G. La Pira 4, I-50121 Firenze, Italy
[2] CNR – Istituto di Geoscienze e Georisorse, Sezione di Firenze, Via G. La Pira 4, I-50121 Firenze, Italy
[3] Dipartimento di Geoscienze, Università degli Studi di Padova, Via Gradenigo 6, I-35131 Padova, Italy
[4] Museo di Mineralogia, Università degli Studi di Padova, Palazzo Cavalli, Via Matteotti 30, I-35121, Padova, Italy
[5] CNR – Istituto di Geoscienze e Georisorse, Sezione di Padova, Via Gradenigo 6, I-35131, Padova, Italy
[6] Pfarrbrunnenstrasse 18, D-66578 Schiffweiler, Germany

[*Received 7 June 2012; Accepted 23 July 2012; Associate Editor: Stuart Mills*]

ABSTRACT

Raberite, ideally $Tl_5Ag_4As_6SbS_{15}$, is a new mineral from Lengenbach quarry in the Binn Valley, Valais, Switzerland. It occurs very rarely as euhedral crystals up to 150 μm across associated with yellow needle-like smithite, realgar, hatchite and probable trechmannite, edenharterite, jentschite and two unidentified sulfosalts. Raberite is opaque with a metallic lustre and has a dark brown–red streak. It is brittle with a Vickers hardness (VHN_{10}) of 52 kg mm^{-2} (range 50–55) corresponding to a Mohs hardness of 2½–3. In reflected light raberite is moderately bireflectant and very weakly pleochroic from light grey to a slightly greenish grey. It is very weakly anisotropic with greyish to light blue rotation tints between crossed polars. Internal reflections are absent. Reflectance percentages for the four COM wavelengths [listed as R_{min}, R_{max}, (λ)] are 30.6, 31.8 (471.1 nm), 28.1, 29.3 (548.3 nm), 27.1, 28.0 (586.6 nm), and 25.8, 26.9 (652.3 nm).

Raberite is triclinic, space group $P\bar{1}$, with a = 8.920(1), b = 9.429(1), c = 20.062(3) Å, α = 79.66(1), β = 88.84(1), γ = 62.72(1)º, V = 1471.6(4) $Å^3$ and Z = 2. The crystal structure [R_1 = 0.0827 for 2110 reflections with $I > 2\sigma(I)$] consists of columns of nine-coordinate Tl atoms forming irregular polyhedra extending along [001] and forming sheets parallel to (010). The columns are decorated by corner-sharing MS_3 pyramids (M = As, Sb) and linked by AgS_3 triangles. Of the seven M positions, one is dominated by Sb and the others by As; the mean M–S bond distances reflect As ↔ Sb substitution at these sites.

The eight strongest lines in the powder diffraction pattern [d_{calc} in Å (I) (hkl)] are: 3.580 (100) ($1\bar{1}3$); 3.506 (58) ($\bar{1}\bar{2}3$); 3.281 (73) (006); 3.017 (54) ($\bar{1}23$); 3.001 (98) (133); 2.657 (51) (226); 2.636 (46) (300); 2.591 (57) (330). A mean of 9 electron microprobe analyses gave Tl 39.55(13), Ag 18.42(8), Cu 0.06(2), As 17.08(7), Sb 5.61(6), S 19.15(11); total 99.87 wt.%, which corresponds to $Tl_{4.85}Ag_{4.28}Cu_{0.02}As_{5.72}Sb_{1.16}S_{14.97}$ with 31 atoms per formula unit. The new mineral has been approved by the IMA-CNMNC Commission (IMA 2012-017) and is named for Thomas Raber, an expert on Lengenbach minerals.

Keywords: raberite, new mineral, Tl-sulfosalts, crystal structure, Lengenbach, Switzerland.

Introduction

Lengenbach quarry in the Binn Valley, Canton Valais, Switzerland is one of the world's premiere localities for Tl-bearing sulfosalts. A considerable number of thallium-bearing minerals have been

* E-mail: luca.bindi@unifi.it
DOI: 10.1180/minmag.2012.076.5.07

reported from the quarry; it is the type locality for imhofite, $Tl_3As_{7.67}S_{13}$ (Burry *et al.*, 1965); erniggliite, $SnTl_2(AsS_3)_2$ (Graeser *et al.*, 1992); edenharterite, $TlPbAs_3S_6$ (Graeser and Schwander, 1992); stalderite, $TlCuZn_2(AsS_3)_2$ (Graeser *et al.*, 1995); jentschite, $TlPbAs_2SbS_6$ (Graeser and Edenharter, 1997); sicherite, $TlAg_2As_3S_6$ (Graeser *et al.*, 2001); gabrielite, $Tl_2AgCu_2As_3S_7$ (Graeser *et al.*, 2006); and the recently described species dalnegroite, $Tl_{5-x}Pb_{2x}(As,Sb)_{21-x}S_{34}$ (x~1) (Nestola *et al.*, 2010).

Raberite was visually identified as a possible new species in 2008 by one of the authors (ME); investigations in 2009 by scanning electron microscopy (Thomas Raber, pers. comm.) and X-ray diffraction (Stefan Graeser, pers. comm.) provided confirmation. The specimen containing raberite was collected in 1992 from the realgar-rich zone (the so-called zone 1; Graeser *et al.*, 2008) in the quarry. The association of raberite with yellow fibrous smithite (Fig. 1), has allowed us to identify the precise position in the Triassic dolomite where the specimen originated. Yellow fibrous smithite has only been found in a realgar-rich zone that was worked at the very beginning of the 'New Lengenbach' quarry (where operations started in 1987). The dolomite in that zone has a saccharoidal texture and the associated sulfides and sulfosalts occur in pore spaces. Pyrite is of variable abundance. Minerals associated with raberite are yellow smithite, realgar, hatchite; probable trechmannite, edenharterite and jentschite, and two unidentified sulfosalts.

Raberite has been approved as a new mineral by the Commission on New Minerals, Nomenclature and Classification of the IMA (proposal 2012-017). The name honours Dr Thomas Raber (b. 1966), a well known expert on Lengenbach minerals for more than 20 years. He has published many articles about Lengenbach minerals and is currently Vice-President of the FGL (Forschungsgemeinschaft Lengenbach; literally: research community Lengenbach). Holotype material is deposited in the mineralogical collections of the Museum of Mineralogy of the Department of Geosciences at the University of Padova (Italy), under catalogue number MMP M11420. To our knowledge, raberite has no synthetic or natural analogues.

Physical and optical properties

Raberite crystallizes very rarely as euhedral elongated black crystals up to ~0.15 mm long on hatchite/wallisite in association with yellowish fibrous smithite (Fig. 1). It does not contain inclusions or intergrowths of other minerals. Raberite has a dark brown–red streak. It is opaque in transmitted light with a metallic lustre. No cleavage was observed and the fracture is uneven. The density calculated from the empirical formula (see below) is 5.649 g cm^{-3}. Unfortunately, the density could not be measured because of the small grain size and absence of suitable heavy liquids. Micro-indentation measurements carried out with a VHN load of 10 g give a mean value of 52 kg mm^{-2} (range: 50–55) corresponding to a Mohs hardness of 2½–3.

In plane-polarized incident light, raberite is dark grey, moderately bireflectant and very weakly pleochroic from light grey to a slightly greenish grey. It is very weakly anisotropic with greyish to light-blue rotation tints between crossed polars. There are no internal reflections and there is no optical evidence of growth zonation.

Reflectance measurements were performed in air using a Zeiss microphotometer (MPM-200) equipped with a MSP-20 system processor on a Zeiss Axioplan ore microscope. The filament temperature was approximately 3350 K. An interference filter was set to the four wavelengths recommended by the Commission on Ore Microscopy (COM). Measurements were taken

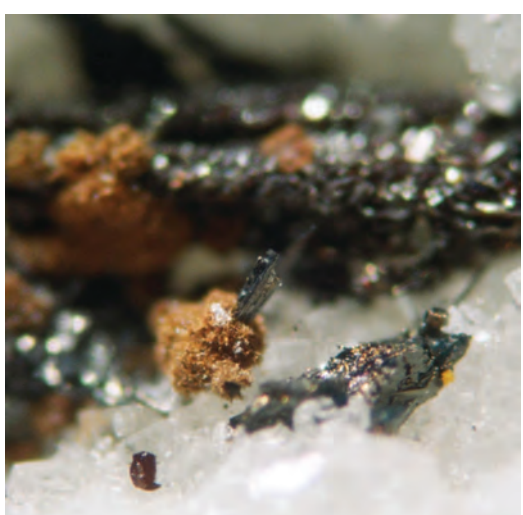

FIG. 1. Black euhedral raberite with yellowish fibrous smithite on a dolomite matrix (white). The picture is 1 mm across.

from a 0.1 mm diameter spot on the specimen and a standard (SiC) in the same focussing conditions. Reflectance percentages [listed as R_{min}, R_{max}, (λ)] are as follows: 30.6, 31.8 (471.1 nm); 28.1, 29.3 (548.3 nm); 27.1, 28.0 (586.6 nm); and 25.8, 26.9 (652.3 nm).

X-ray crystallography and crystal-structure determination

A small crystal fragment ($65 \times 60 \times 55$ μm) was selected for study on a STOE-STADI IV CCD single-crystal diffractometer (Table 1). No systematic absences were observed in the initial dataset, leading to a choice of space groups of $P1$ or $P\bar{1}$. Statistical tests on the distribution of $|E|$ values ($|E^2-1| = 0.868$) indicated the presence of an inversion centre, suggesting that $P\bar{1}$ was the appropriate choice. The positions of most of the atoms (Tl, Ag and As/Sb atoms) were determined by direct methods using *SHELXS* (Sheldrick, 2008). A least-squares refinement on F^2 using these heavy atom positions and isotropic displacement parameters produced an R factor of 0.216. Three-dimensional difference-Fourier synthesis yielded the positions of the remaining sulfur atoms. The program *SHELXL* (Sheldrick, 2008) was used to refine the structure. The occupancy of

TABLE 1. Crystallographic data and refinement parameters for raberite.

Crystal data	
Ideal formula	$Tl_5Ag_4As_6SbS_{15}$
Crystal system	Triclinic
Space group	$P\bar{1}$
Unit-cell parameters, a, b, c (Å)	8.920(1), 9.429(1), 20.062(3)
Unit-cell angles α, β, γ (º)	79.66(1), 88.84(1), 62.72(1)
Unit-cell volume (Å^3)	1471.6(4)
Z	2
Crystal size (mm)	$0.065 \times 0.060 \times 0.055$
Data collection	
Diffractometer	STOE-STADI IV CCD
Temperature (K)	298(3)
Radiation, wavelength (Å)	Mo$K\alpha$, 0.71073
2θ max for data collection (º)	59.66
Crystal–detector distance (mm)	50
h, k, l ranges	−8 to 12, −12 to 13, −26 to 28
Axis, frames, width (º), time per frame (s)	ω, 570, 1.00, 40
Total reflections collected	14,126
Unique reflections (R_{int})	8174 (0.124)
Unique reflections $I > 2s(I)$	2110
Data completeness to θ_{max} (%)	99.4
Absorption correction method	*X-RED* and *X-SHAPE*
Structure refinement	
Refinement method	Full-matrix least-squares on I
Data/restraints/parameters	2110/0/286
R_1 [$I > 2\sigma(I)$], wR_2 [$I > 2\sigma(I)$]	0.0827, 0.1788
R_1 all, wR_2 all	0.1088, 0.2140
Goodness-of-fit on F^2	0.752
Largest diff. peak and hole (e$^-$ Å^{-3})	3.05, −7.78

Refinement parameters are as follows:

$R_{int} = (n/n-1)^{1/2}[F_o^2 - F_o\,(\text{mean})^2]/\Sigma F_o^2$

$R_1 = \Sigma||F_o| - |F_c||/\Sigma|F_o|$; $wR_2 = \{\Sigma[w(F_o^2 - F_c^2)^2]/\Sigma[w(F_o^2)^2]\}^{1/2}$;

$\text{GooF} = \{\Sigma[w(F_o^2 - F_c^2)^2]/(n-p)\}^{1/2}$

where n is the number of reflections and p is the number of refined parameters.

all the sites, except the *M* sites (see below), was left free to vary (Tl *vs*. vacancy; Ag *vs*. vacancy; S *vs*. vacancy) and then fixed to the resulting value. The occupancy of the seven *M* sites (Table 2) was refined using the curves of As *vs*. Sb. The refined values are given in Table 2. Neutral scattering curves for Tl, Ag, As, Sb and S were taken from the *International Tables for X-ray Crystallography* (Ibers and Hamilton, 1974). At the last stage of the refinement, with anisotropic atomic displacement parameters for all atoms and no constraints, the residuals settled at $R = 0.0827$ for 2110 observed reflections [$2\sigma(I)$ level] and 286 parameters, and at $R = 0.1088$ for all 8174 independent reflections. Experimental details and *R* values are listed in Table 1. Fractional atom coordinates and isotropic displacement parameters are reported in Table 2 (anisotropic ADPs can be found in the accompanying CIF). Bond distances are given in Table 3. Calculated X-ray powder diffraction data, computed using the atom coordinates and occupancies reported in Table 2, are listed in Table 4, with the measured pattern. Structure factors have been deposited with the Principal Editor of *Mineralogical Magazine* and are available at http://www. minersoc.org/pages/e_journals/dep_mat_mm.html.

Chemical composition

A preliminary chemical analysis by energy-dispersive spectrometry was performed using a

TABLE 2. Atoms, site occupancies, fractional atom coordinates (Å) and isotropic atomic displacement parameters (Å^2) for raberite.*

Site	Site occupancy	*x/a*	*y/b*	*z/c*	U_{iso}
Tl1	$Tl_{1.00}$	0.8636(2)	0.6454(2)	0.40728(8)	0.0385(4)
Tl2	$Tl_{1.00}$	0.4966(2)	0.6427(2)	0.23847(9)	0.0467(5)
Tl3	$Tl_{1.00}$	0.1081(2)	0.3673(2)	0.27428(8)	0.0373(4)
Tl4	$Tl_{1.00}$	0.1239(2)	0.3643(2)	−0.07844(9)	0.0496(5)
Tl5	$Tl_{1.00}$	0.5026(2)	0.3594(2)	0.43830(8)	0.0382(4)
Ag1	$Ag_{1.00}$	0.4460(4)	0.0195(4)	0.4081(2)	0.054(1)
Ag2	$Ag_{1.00}$	0.4806(4)	0.0479(5)	0.0698(2)	0.078(1)
Ag3	$Ag_{1.00}$	−0.4636(4)	0.0017(4)	0.2397(2)	0.068(1)
Ag4	$Ag_{1.00}$	0.3784(4)	0.3520(5)	0.1620(2)	0.069(2)
M1	$As_{0.73(3)}Sb_{0.27}$	−0.0113(4)	0.8450(4)	0.2238(2)	0.028(1)
M2	$Sb_{0.63(3)}As_{0.37}$	0.2022(3)	0.8436(4)	0.0485(2)	0.037(1)
M3	$As_{0.94(3)}Sb_{0.06}$	0.0093(4)	0.1649(4)	0.4491(2)	0.027(1)
M4	$As_{0.90(3)}Sb_{0.10}$	0.1848(4)	0.8342(4)	0.3858(2)	0.026(1)
M5	$As_{0.98(3)}Sb_{0.02}$	0.1041(4)	0.1270(5)	0.1402(2)	0.031(1)
M6	$As_{0.86(3)}Sb_{0.14}$	0.6583(4)	0.3139(5)	0.0989(2)	0.038(2)
M7	$As_{1.00}$	0.7797(4)	0.1143(5)	0.3188(2)	0.0290(9)
S1	$S_{1.00}$	0.188(1)	0.269(1)	0.4276(5)	0.033(2)
S2	$S_{1.00}$	0.175(1)	0.671(1)	0.1534(5)	0.034(2)
S3	$S_{1.00}$	0.175(1)	0.659(1)	0.3212(4)	0.026(2)
S4	$S_{1.00}$	−0.200(1)	0.741(1)	0.2416(5)	0.032(2)
S5	$S_{1.00}$	0.742(1)	0.003(1)	0.4225(5)	0.030(2)
S6	$S_{1.00}$	−0.170(1)	0.314(1)	0.3506(5)	0.028(2)
S7	$S_{1.00}$	0.507(1)	0.259(1)	0.2823(5)	0.036(2)
S8	$S_{1.00}$	0.463(1)	0.755(1)	0.3954(5)	0.035(2)
S9	$S_{1.00}$	0.205(1)	0.292(1)	0.0888(5)	0.038(3)
S10	$S_{1.00}$	−0.170(1)	0.334(1)	0.5160(4)	0.024(2)
S11	$S_{1.00}$	−0.148(1)	0.312(1)	0.1735(5)	0.030(2)
S12	$S_{1.00}$	0.245(1)	0.019(1)	0.2420(5)	0.035(2)
S13	$S_{1.00}$	0.250(1)	0.610(1)	0.0014(5)	0.037(2)
S14	$S_{1.00}$	0.245(1)	0.952(1)	−0.0967(5)	0.042(3)
S15	$S_{1.00}$	0.481(1)	0.782(1)	0.0766(5)	0.036(3)

* All the atoms are in the 2*i* position.

TABLE 3. Selected bond distances (Å) for raberite.

Tl1–S1	3.36(1)	Tl2–S2	3.25(1)	Tl3–S1	3.05(1)
Tl1–S1	3.52(1)	Tl2–S3	3.24(1)	Tl3–S2	3.66(1)
Tl1–S3	3.28(1)	Tl2–S4	3.25(1)	Tl3–S3	3.36(1)
Tl1–S4	3.27(1)	Tl2–S6	3.58(1)	Tl3–S4	3.28(1)
Tl1–S5	3.11(1)	Tl2–S7	3.53(1)	Tl3–S6	3.07(1)
Tl1–S6	3.64(1)	Tl2–S8	3.46(1)	Tl3–S7	3.22(1)
Tl1–S8	3.23(1)	Tl2–S11	3.70(1)	Tl3–S9	3.92(1)
Tl1–S10	3.46(1)	Tl2–S12	3.22(1)	Tl3–S11	3.36(1)
Tl1–S10	3.26(1)	Tl2–S15	3.26(1)	Tl3–S12	3.13(1)
<Tl1–S>	**3.35**	**<Tl2–S>**	**3.39**	**<Tl3–S>**	**3.34**
Tl4–S2	3.26(1)	Tl5–S1	3.31(1)	Ag1–S1	2.51(1)
Tl4–S4	3.55(1)	Tl5–S3	3.51(1)	Ag1–S5	2.59(1)
Tl4–S9	3.33(1)	Tl5–S5	3.12(1)	Ag1–S8	2.49(1)
Tl4–S9	3.20(1)	Tl5–S6	3.28(1)	**<Ag1–S>**	**2.53**
Tl4–S11	3.40(1)	Tl5–S7	3.42(1)		
Tl4–S13	3.61(1)	Tl5–S8	3.53(1)	Ag2–S9	2.57(1)
Tl4–S13	3.57(1)	Tl5–S8	3.29(1)	Ag2–S14	2.52(1)
Tl4–S14	3.61(1)	Tl5–S10	3.23(1)	Ag2–S15	2.49(1)
Tl4–S15	3.14(1)	Tl5–S10	3.31(1)	**<Ag2–S>**	**2.53**
<Tl4–S>	**3.41**	**<Tl5–S>**	**3.33**		
Ag3–S4	2.50(1)	Ag4–S2	2.68(1)	*M*1–S2	2.39(1)
Ag3–S7	2.61(1)	Ag4–S7	2.52(1)	*M*1–S3	2.43(1)
Ag3–S12	2.53(1)	Ag4–S9	2.46(1)	*M*1–S4	2.30(1)
<Ag3–S>	**2.55**	**<Ag4–S>**	**2.55**	**<*M*1–S>**	**2.37**
*M*2–S2	2.50(1)	*M*3–S1	2.22(1)	*M*4–S3	2.31(1)
*M*2–S13	2.40(1)	*M*3–S6	2.35(1)	*M*4–S8	2.24(1)
*M*2–S15	2.33(1)	*M*3–S10	2.29(1)	*M*4–S10	2.34(1)
<*M*2–S>	**2.41**	**<*M*3– S>**	**2.29**	**<*M*4– S>**	**2.30**
*M*5–S9	2.23(1)	*M*6–S11	2.30(1)	*M*7–S5	2.25(1)
*M*5–S11	2.31(1)	*M*6–S13	2.28(1)	*M*7–S6	2.32(1)
*M*5–S12	2.23(1)	*M*6–S14	2.26(1)	*M*7–S7	2.23(1)
<*M*5–S>	**2.26**	**<*M*6– S>**	**2.28**	**<*M*7– S>**	**2.27**

JEOL-5610 LV SEM at the Museum of Natural History of Milan. The chemical composition was subsequently determined by wavelength-dispersive spectrometry (WDS) using a CAMECA-CAMEBAX electron microprobe. The major- and minor-element composition was determined at 20 kV accelerating voltage and 20 nA beam current with a 1 μm beam size and 15 s counting times. The following lines and standards were used in the WDS analyses: Tl*M*α, Ag*L*α, Cu*K*α, As*L*α, Sb*L*α and S*K*α; with synthetic Tl_2Se (Tl), elemental Ag (Ag), elemental Cu (Cu), synthetic AsGa (As), stibnite (Sb) and sphalerite (S), respectively. The crystal fragment was homogeneous to within analytical error. The average chemical compositions (9 analyses on different spots) together with wt.% ranges of elements are reported in Table 5. On the basis of 31 atoms, the empirical formula of raberite is $Tl_{4.85}Ag_{4.28}Cu_{0.02}As_{5.72}Sb_{1.16}S_{14.97}$. The simplified ideal formula is $Tl_5Ag_4As_6SbS_{15}$, which requires Tl 40.79, Ag 17.22, As 17.94, Sb 4.86, S 19.19; total 100.00 wt.%.

Results and discussion

In the crystal structure of raberite (Fig. 2) columns of nine-coordinate Tl atoms forming irregular polyhedra extend along [001] and form sheets parallel to (010). The Tl atoms in the columns are interrupted by Ag4 and *M*6 positions (i.e. every 5 Tl positions there is the couple

TABLE 4. X-ray powder diffraction data for raberite.

— Calculated* —			– Measured‡ –		— Calculated* —			– Measured‡ –	
hkl	d_{calc} (Å)	I_{calc} (%)	d_{obs} (Å)	I_{meas} (%)	*hkl*	d_{calc} (Å)	I_{calc} (%)	d_{obs} (Å)	I_{meas} (%)
001	19.687	8			$\bar{2}\bar{2}6$	2.380	6		
110	7.772	19			036	2.336	7		
103	4.883	14			$\bar{2}23$	2.334	6		
$\bar{1}\bar{1}3$	4.760	7			140	2.261	8		
210	4.458	12			$\bar{3}10$	2.229	10		
$\bar{1}13$	4.139	14			$\bar{1}\bar{3}5$	2.226	6		
123	4.136	27			336	2.153	9		
020	4.112	8			423	2.126	8		
200	3.954	16			$2\bar{1}6$	2.107	17		
220	3.886	31			$\bar{4}\bar{2}3$	2.096	10		
015	3.850	7			109	2.071	8		
213	3.729	37			$\bar{2}\bar{3}6$	2.057	5		
$\bar{2}\bar{1}3$	3.647	19	3.650	20	040	2.056	13		
$1\bar{1}3$	**3.580**	**100**	**3.578**	**100**	$\bar{1}\bar{1}9$	2.047	11		
223	3.520	26			229	2.004	8		
$\bar{1}\bar{2}3$	**3.506**	**58**	**3.476**	**75**	306	1.987	17		
$\bar{2}03$	3.498	32			$\bar{2}09$	1.974	8		
$\bar{2}\bar{2}2$	3.484	13			139	1.962	8		
006	**3.281**	**73**	**3.278**	**80**	$\bar{1}29$	1.955	8		
016	3.271	33	3.267	30	$\bar{3}\bar{3}6$	1.931	11		
$\bar{2}\bar{1}4$	3.266	5			$0\bar{3}6$	1.930	12		
$\bar{2}04$	3.195	16			$\bar{2}33$	1.894	9		
116	3.151	11			444	1.880	5		
$\bar{1}\bar{2}4$	3.112	8			$1\bar{1}9$	1.878	7		
$\bar{1}20$	3.108	28	3.086	30	253	1.875	11		
130	3.066	21	3.050	20	$\bar{1}\bar{2}9$	1.857	6		
$\bar{2}12$	3.027	10			250	1.853	5		
$\bar{1}23$	**3.017**	**54**	**2.996**	**50**	$\bar{4}\bar{1}6$	1.829	6		
133	**3.001**	**98**	**2.994**	**85**	$2\bar{2}6$	1.790	8		
$\bar{1}\bar{1}6$	2.909	26	2.880	30	$\bar{2}36$	1.763	6		
311	2.899	12			446	1.760	8		
$0\bar{1}6$	2.865	21	2.853	15	256	1.756	12		
$\bar{3}\bar{2}1$	2.859	8			$\bar{2}\bar{4}6$	1.753	6		
322	2.839	5			$\bar{4}10$	1.747	6		
017	2.832	16			149	1.747	7		
$\bar{3}\bar{2}2$	2.752	9			319	1.745	7		
030	2.742	43	2.729	25	$\bar{1}39$	1.745	8		
$\bar{3}\bar{1}3$	2.690	13			$2\bar{3}3$	1.735	12		
216	2.673	14			453	1.716	5		
313	2.669	31			$\bar{1}\bar{4}6$	1.715	5		
226	**2.657**	**51**	**2.665**	**75**	$\bar{2}\bar{5}3$	1.704	6		
$1\bar{2}3$	2.638	13	2.638	15	$01\underline{12}$	1.671	9		
300	**2.636**	**46**	**2.624**	**40**	$1\bar{4}3$	1.658	6		
$\bar{2}06$	2.618	28			$4\bar{1}3$	1.647	9		
$\bar{2}\bar{1}6$	2.613	12			$02\underline{12}$	1.635	6		
$\bar{3}\bar{2}3$	2.609	11			$\bar{4}\bar{5}3$	1.604	7		
$\bar{1}\bar{3}3$	2.598	13			056	1.598	11		
330	**2.591**	**57**	**2.585**	**50**	526	1.564	7		
136	2.483	21	2.478	25	$03\underline{12}$	1.544	5		
$\bar{1}\bar{2}6$	2.481	6			$\bar{5}\bar{3}6$	1.529	9		
$\bar{1}26$	2.480	25	2.476	20	$\bar{4}09$	1.521	6		
217	2.405	6							

TABLE 5. Electron microprobe analyses (means, ranges and standard deviations) and atomic ratios (on the basis of 31 atoms per formula unit) for raberite.

Element	Mean (wt.%)	Range	SD	Atomic ratio
Tl	39.55	38.44–39.76	0.13	4.85
Ag	18.42	18.30–20.30	0.08	4.28
Cu	0.06	0.00–0.07	0.02	0.02
As	17.08	16.34–17.21	0.07	5.72
Sb	5.61	4.71–5.90	0.06	1.16
S	19.15	18.43–19.20	0.11	14.97
Total	99.87	98.55–100.21	31.00	

Ag4–*M*6, which is at a distance of 2.68 Å). The columns are decorated by corner-sharing MS_3 pyramids (M = As, Sb) and linked by AgS_3 triangles (Ag1, Ag2, and Ag3 positions). The Tl atoms are in an irregular coordination environment (Fig. 3) and the distances to the surrounding sulfur atoms are variable (Table 3). If we use distances <3.40 Å to represent bonds (continuous

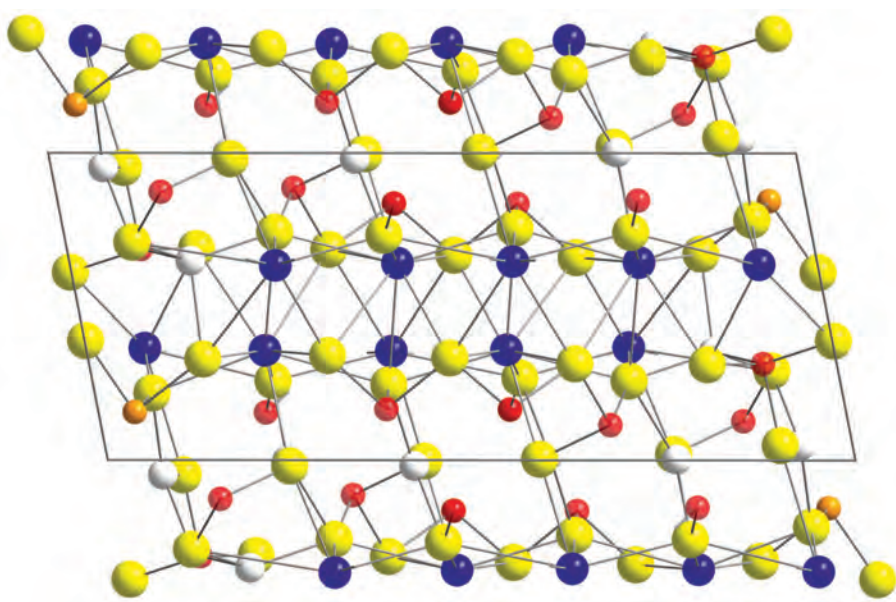

FIG. 2. The crystal structure of raberite projected down [100]. The horizontal direction is the *c* axis; Tl, Ag, As, Sb, and S atoms are represented by blue, white, red, orange and yellow spheres, respectively. The unit cell is outlined.

Footnotes to Table 4 (*facing page*)
The eight strongest lines are listed in bold.
* The calculated powder pattern with indexing for raberite on the basis of a = 8.920(1) Å, b = 9.429(1), c = 20.062(3) Å, α = 79.66(1), β = 88.84(1), γ = 62.72(1), and with the atom coordinates and occupancies reported in Table 2.
‡ The measured powder pattern for raberite obtained with a CCD-equipped single crystal diffractometer (Cu$K\alpha$ radiation). The refined unit-cell parameters from these data are as follows: a = 8.8670(9) Å, b = 9.3796(8), c = 19.989(2) Å, α = 79.690(8), β = 89.226(8), γ = 62.853(8), V = 1451.0(2) Å^3.

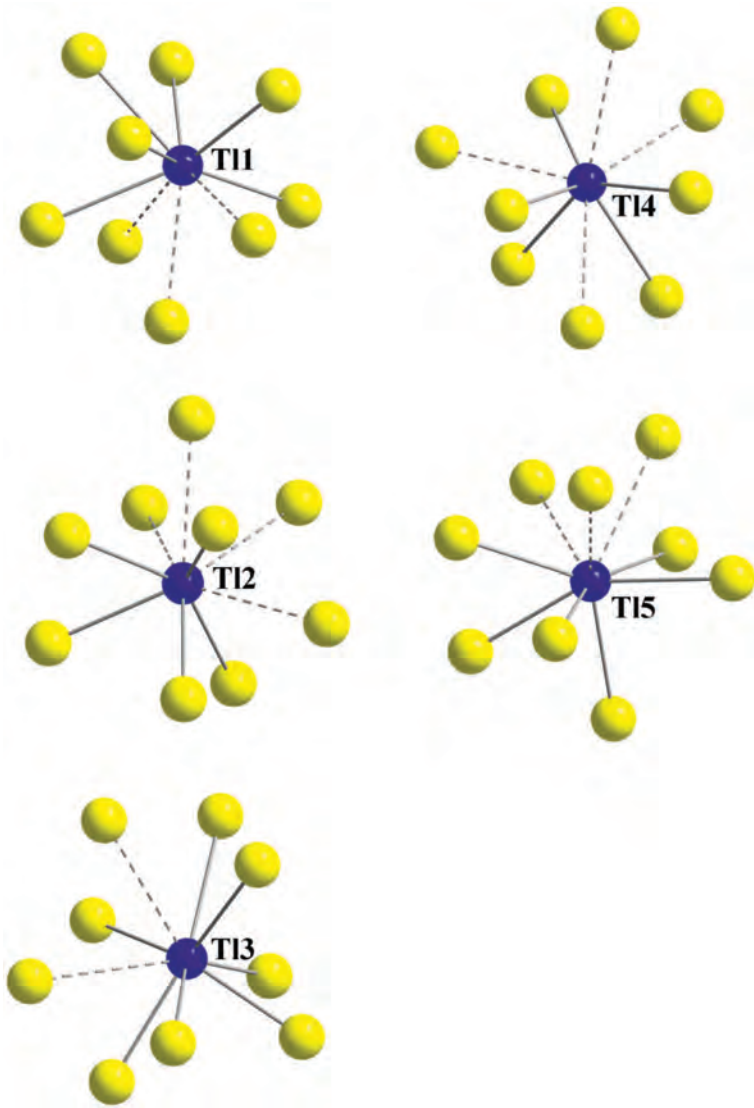

FIG. 3. Coordination environments of Tl atoms. Bond distances longer than 3.40 Å are represented by dashed lines; Tl and S atoms are blue and yellow spheres, respectively.

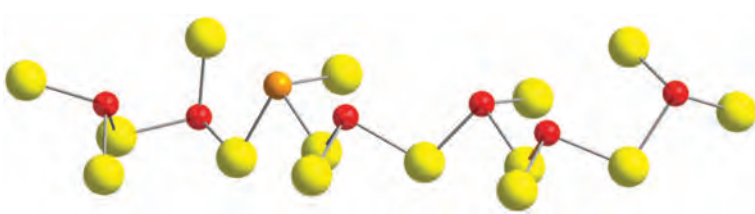

FIG. 4. Corner-sharing *M* atoms. The As, Sb, and S atoms are red, orange and yellow spheres, respectively.

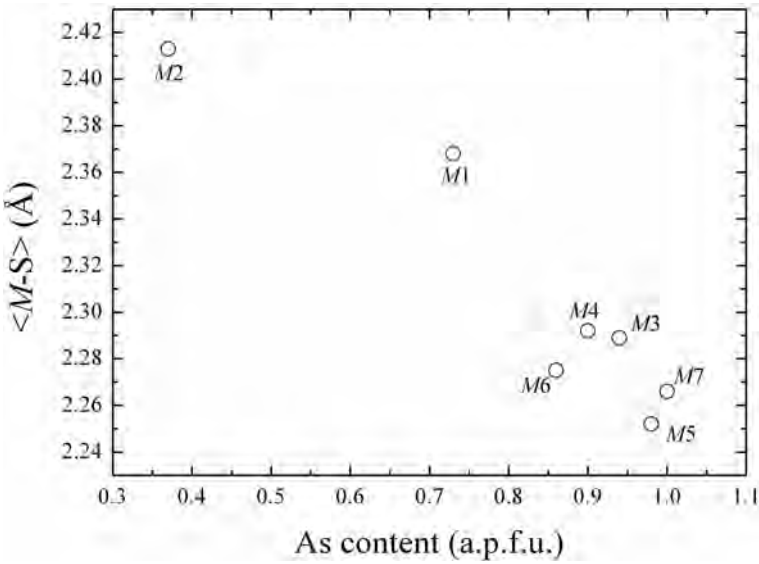

FIG. 5. The mean $M-S$ bond distance (Å) plotted against refined As content (a.p.f.u.) at the different sites.

bonds in Fig. 3), Tl2 and Tl4 are five coordinate, Tl1 and Tl5 are six coordinate and Tl3 is seven coordinate. The Tl atoms are, however, nine coordinate if longer distances (up to 4 Å) are included (dashed bonds in Fig. 3). The mean bond distances for the Tl-polyhedra are in the range 3.33–3.41 Å, which is in excellent agreement with the sum of the ionic radii of $^{VI}Tl^{+}$ and S^{2-} (3.34 Å; Shannon, 1976), suggesting that the bonding of thallium is largely ionic in this structure. The Tl–S distances in raberite are similar to Tl sites (Tl1 and Tl3) in gabrielite, $Tl_2AsCu_2As_3S_7$ (3.38–3.49 Å; Balić-Žunić *et al.*, 2006) and sicherite, $TlAg_2(As,Sb)_3S_6$ (3.34 Å; Graeser *et al.*, 2001). The Ag–S distances are in the range 2.53–2.55 Å, which is similar to those reported for different polytypes of pearceite–polybasite (2.50–2.56 Å; Bindi *et al.*, 2006, 2007; Evain *et al.*, 2006). The *M* atoms, forming corner-sharing rods along the *c* axis (Fig. 4), are three coordinate. They occupy the top of a pyramid with 3 sulfur atoms forming the base. Bond distances are similar to those reported for silver thioantimonates and silver sulfides. Of the seven corner-sharing *M* positions (Table 2), only one (*M*2) contains more Sb than As. The mean $M-S$ bond distances reflect the As ↔ Sb substitution that occurs at these sites (Fig. 5).

The Ag4–*M*6 short contact (i.e. 2.68 Å) is worthy of consideration. In general, all the Ag

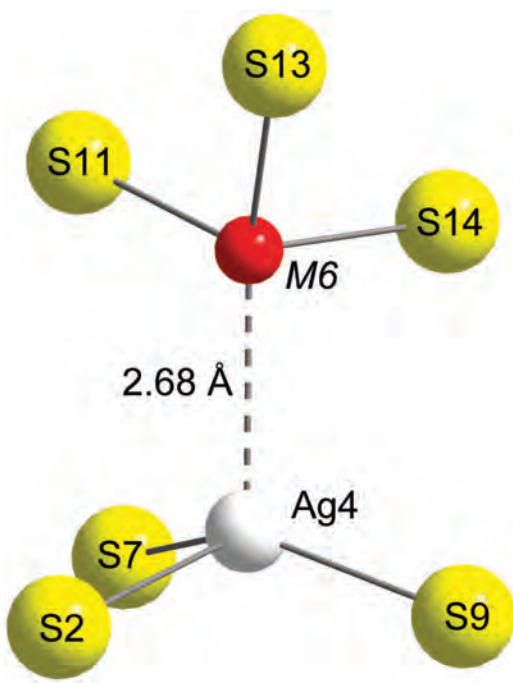

FIG. 6. Crystal-chemical environment of the couple Ag4–*M*6. The contact between the two atoms is depicted using a dashed line. The Ag, As and S atoms are white, red and yellow spheres, respectively.

TABLE 6. Bond valences (vu) for raberite.*

Site	BV	Site	BV
Tl1	1.12(2)	S1	2.11(2)
Tl2	1.02(2)	S2	2.22(2)
Tl3	1.30(2)	S3	2.20(2)
Tl4	0.98(2)	S4	1.96(2)
Tl5	1.13(2)	S5	1.77(2)
Ag1	1.00(2)	S6	2.22(2)
Ag2	1.00(2)	S7	2.05(2)
Ag3	0.95(2)	S8	1.98(2)
Ag4	0.96(2)	S9	2.14(2)
*M*1	2.74(2)	S10	2.39(2)
*M*2	3.06(2)	S11	2.04(2)
*M*3	3.04(2)	S12	1.83(2)
*M*4	3.03(2)	S13	2.23(2)
*M*5	3.19(2)	S14	1.75(2)
*M*6	3.23(2)	S15	1.96(2)
*M*7	3.06(2)		

* Calculated from the bond valence curves of Brese and O'Keeffe (1991).

atoms are displaced from the centre of the trigonal plane. The direction of the displacement depends on the environment, whereas its extent usually depends on the degree of Ag substitution by a lighter element such as Cu. In raberite, the Ag positions are fully occupied by silver and, in the case of the Ag4 site, the displacement is toward the adjacent *M*6 with a refined population of $As_{0.86(3)}Sb_{0.14}$. The lone pair of electrons of the latter site points toward the Ag4 atom (Fig. 6). The short Ag–As distance for Ag4–*M*6 might be indicative of a situation in which As plays the role of an anion. This has been hypothesized in synthetic compounds with short Tl–As bond distances (from 2.74 to 2.88 Å) such as $Rb_5TaAs_4Tl_2$ (Huang and Corbett, 1998), a transition-metal Zintl phase which contains the $TaAs_4Tl_2^{5-}$ polyanion.

Bond-valence sums calculated from the curves of Brese and O'Keeffe (1991) are reported in Table 6. They are in excellent agreement with the cation populations assumed in the present study.

Acknowledgements

The manuscript benefited from the revision of S. Graeser, P. Leverett, D. Topa, and Associate Editor S. Mills. The research was supported by "progetto d'Ateneo 2006, University of Padova" to FN. Thanks are due to Dr Federico Pezzotta (Natural History Museum, Milan, Italy) for the use of the scanning electron microscope.

References

Balić-Žunić, T., Makovicky, E., Karanović, L., Poleti, D. and Graeser, S. (2006) The crystal structure of gabrielite, $Tl_2AgCu_2As_3S_7$, a new species of thallium sulfosalt from Lengenbach, Switzerland. *The Canadian Mineralogist*, **44**, 141–158.

Bindi, L., Evain, M. and Menchetti, S. (2006) Temperature dependence of the silver distribution in the crystal structure of natural pearceite, $(Ag,Cu)_{16}(As,Sb)_2S_{11}$. *Acta Crystallographica*, **B62**, 212–219.

Bindi, L., Evain, M. and Menchetti, S. (2007) Complex twinning, polytypism and disorder phenomena in the crystal structures of antimonpearceite and arsenpolybasite. *The Canadian Mineralogist*, **45**, 321–333.

Brese, N.E. and O'Keeffe, M. (1991) Bond-valence parameters for solids. *Acta Crystallographica*, **B47**, 192–197.

Burry, G., Graeser, S., Marumo, F. and Nowacki, W. (1965) Imhofit, ein neues Thallium- Arsensulfosalz aus dem Lengenbach (Binnatal, Kanton Wallis). *Chimia*, **19**, 499–500.

Evain, M., Bindi, L. and Menchetti, S. (2006) Structural complexity in minerals: twinning, polytypism and disorder in the crystal structure of polybasite, $(Ag,Cu)_{16}(Sb,As)_2S_{11}$. *Acta Crystallographica*, **B62**, 447–456.

Graeser, S. and Edenharter, A. (1997) Jentschite ($TlPbAs_2SbS_6$) – a new sulfosalt mineral from Lengenbach, Binntal (Switzerland). *Mineralogical Magazine*, **61**, 131–137.

Graeser, S. and Schwander, H. (1992) Edenharterite ($TlPbAs_3S_6$): a new mineral from Lengenbach, Binntal (Switzerland). *European Journal of Mineralogy*, **4**, 1265–1270.

Graeser, S., Schwander, H., Wulf, R. and Edenharter, A. (1992) Erniggliite ($Tl_2SnAs_2S_6$), a new mineral from Lengenbach, Binntal (Switzerland): description and crystal structure determination based on data from synchrotron radiation. *Schweizerische mineralogische und petrographische Mitteilungen*, **72**, 293–305.

Graeser, S., Schwander, H., Wulf, R. and Edenharter, A. (1995) Stalderite $TlCu(Zn,Fe,Hg)_2As_2S_6$ – a new mineral related to routhierite: description and crystal structure determination. *Schweizerische mineralogische und petrographische Mitteilungen*, **75**, 337–345.

Graeser, S., Berlepsch, P., Makovicky, E. and Balić-Žunić, T. (2001) Sicherite, $TlAg_2(As,Sb)_3S_6$, a new sulfosalt mineral from Lengenbach (Binntal, Switzerland): description and structure determina-

tion. *American Mineralogist*, **86**, 1087–1093.

Graeser, S., Topa, D., Balić-Zunić, T. and Makovicky, E. (2006) Gabrielite, $Tl_2AgCu_2As_3S_7$, a new species of thallium sulfosalt from Lengenbach, Binntal, Switzerland. *The Canadian Mineralogist*, **44**, 135–140.

Graeser, S., Cannon, R., Drechsler, E., Raber, T. and Roth, P. (2008) *Faszination Lengenbach Abbau-Forschung-Mineralien 1958–2008*. Kristallographik Verlag, Achberg, Germany.

Huang, D.P. and Corbett, J.D. (1998) $A_5TaAs_4Tl_2$ (A = Rb, K). Transition-metal Zintl phases with a novel complex ion: synthesis, structure, and bonding. *Inorganic Chemistry*, **37**, 4006–4010.

Ibers, J.A. and Hamilton, W.C. (editors) (1974) *International Tables for X-ray Crystallography*, volume. IV. Kynock Press, Birmingham, UK.

Nestola, F., Guastoni, A., Bindi, L. and Secco L. (2010) Dalnegroite, $Tl_{5-x}Pb_{2x}(As,Sb)_{21-x}S_{34}$, a new thallium sulphosalt from Lengenbach quarry, Binntal, Canton Valais, Switzerland. *Mineralogical Magazine*, **73**, 1027–1032.

Shannon, R.D. (1976) Revised effective ionic radii and systematic studies of interatomic distances in halides and chalcogenides. *Acta Crystallographica*, **A32**, 751–767.

Sheldrick, G.M. (2008) A short history of *SHELX*. *Acta Crystallographica*, **A64**, 112–122.

```
data_shelxl

_audit_creation_method            SHELXL-97
_chemical_name_systematic
;
 ?
;
_chemical_name_common             ?
_chemical_melting_point           ?
_chemical_formula_moiety          ?
_chemical_formula_sum
 'Ag4 As7 Cu0 S15 Sb0 Tl5'
_chemical_formula_weight          2458.67

loop_
 _atom_type_symbol
 _atom_type_description
 _atom_type_scat_dispersion_real
 _atom_type_scat_dispersion_imag
 _atom_type_scat_source
 'Ag'  'Ag'  -0.8971   1.1015
 'International Tables Vol C Tables 4.2.6.8 and 6.1.1.4'
 'As'  'As'   0.0499   2.0058
 'International Tables Vol C Tables 4.2.6.8 and 6.1.1.4'
 'S'  'S'   0.1246   0.1234
 'International Tables Vol C Tables 4.2.6.8 and 6.1.1.4'
 'Tl'  'Tl'  -2.8358   9.6688
 'International Tables Vol C Tables 4.2.6.8 and 6.1.1.4'
 'Sb'  'Sb'  -0.5866   1.5461
 'International Tables Vol C Tables 4.2.6.8 and 6.1.1.4'
 'Cu'  'Cu'   0.3201   1.2651
 'International Tables Vol C Tables 4.2.6.8 and 6.1.1.4'

_symmetry_cell_setting            ?
_symmetry_space_group_name_H-M    ?

loop_
 _symmetry_equiv_pos_as_xyz
 'x, y, z'
 '-x, -y, -z'

_cell_length_a                    8.9200(10)
_cell_length_b                    9.4290(10)
_cell_length_c                    20.062(3)
_cell_angle_alpha                 79.660(10)
_cell_angle_beta                  88.840(10)
_cell_angle_gamma                 62.720(10)
_cell_volume                      1471.6(3)
_cell_formula_units_Z             2
_cell_measurement_temperature     293(2)
_cell_measurement_reflns_used     ?
_cell_measurement_theta_min       ?
_cell_measurement_theta_max       ?

_exptl_crystal_description        ?
_exptl_crystal_colour             ?
_exptl_crystal_size_max           ?
_exptl_crystal_size_mid           ?
_exptl_crystal_size_min           ?
```

```
_exptl_crystal_density_meas       ?
_exptl_crystal_density_diffrn     5.549
_exptl_crystal_density_method     'not measured'
_exptl_crystal_F_000              2128
_exptl_absorpt_coefficient_mu     38.741
_exptl_absorpt_correction_type    ?
_exptl_absorpt_correction_T_min   ?
_exptl_absorpt_correction_T_max   ?
_exptl_absorpt_process_details    ?

_exptl_special_details
;
 ?
;

_diffrn_ambient_temperature       293(2)
_diffrn_radiation_wavelength      0.71073
_diffrn_radiation_type            MoK\a
_diffrn_radiation_source          'fine-focus sealed tube'
_diffrn_radiation_monochromator   graphite
_diffrn_measurement_device_type   ?
_diffrn_measurement_method        ?
_diffrn_detector_area_resol_mean  ?
_diffrn_standards_number          ?
_diffrn_standards_interval_count  ?
_diffrn_standards_interval_time   ?
_diffrn_standards_decay_%         ?
_diffrn_reflns_number             14126
_diffrn_reflns_av_R_equivalents   0.1244
_diffrn_reflns_av_sigmaI/netI     0.3549
_diffrn_reflns_limit_h_min        -8
_diffrn_reflns_limit_h_max        12
_diffrn_reflns_limit_k_min        -12
_diffrn_reflns_limit_k_max        13
_diffrn_reflns_limit_l_min        -26
_diffrn_reflns_limit_l_max        28
_diffrn_reflns_theta_min          2.84
_diffrn_reflns_theta_max          29.83
_reflns_number_total              8174
_reflns_number_gt                 2110
_reflns_threshold_expression      >2sigma(I)

_computing_data_collection        ?
_computing_cell_refinement        ?
_computing_data_reduction         ?
_computing_structure_solution     ?
_computing_structure_refinement   'SHELXL-97 (Sheldrick, 1997)'
_computing_molecular_graphics     ?
_computing_publication_material   ?

_refine_special_details
;
 Refinement of F^2^ against ALL reflections.  The weighted R-factor wR and
 goodness of fit S are based on F^2^, conventional R-factors R are based
 on F, with F set to zero for negative F^2^. The threshold expression of
 F^2^ > 2sigma(F^2^) is used only for calculating R-factors(gt) etc. and is
 not relevant to the choice of reflections for refinement.  R-factors based
 on F^2^ are statistically about twice as large as those based on F, and R-
 factors based on ALL data will be even larger.
;
```

```
_refine_ls_structure_factor_coef  Fsqd
_refine_ls_matrix_type            full
_refine_ls_weighting_scheme       calc
_refine_ls_weighting_details
 'calc w=1/[\s^2^(Fo^2^)+(0.0725P)^2^+0.0000P] where P=(Fo^2^+2Fc^2^)/3'
_atom_sites_solution_primary      direct
_atom_sites_solution_secondary    difmap
_atom_sites_solution_hydrogens    geom
_refine_ls_hydrogen_treatment     mixed
_refine_ls_extinction_method      none
_refine_ls_extinction_coef        ?
_refine_ls_number_reflns          8174
_refine_ls_number_parameters      286
_refine_ls_number_restraints      0
_refine_ls_R_factor_all           0.1088
_refine_ls_R_factor_gt            0.0827
_refine_ls_wR_factor_ref          0.2140
_refine_ls_wR_factor_gt           0.1788
_refine_ls_goodness_of_fit_ref    0.752
_refine_ls_restrained_S_all       0.752
_refine_ls_shift/su_max           0.000
_refine_ls_shift/su_mean          0.000

loop_
 _atom_site_label
 _atom_site_type_symbol
 _atom_site_fract_x
 _atom_site_fract_y
 _atom_site_fract_z
 _atom_site_U_iso_or_equiv
 _atom_site_adp_type
 _atom_site_occupancy
 _atom_site_symmetry_multiplicity
 _atom_site_calc_flag
 _atom_site_refinement_flags
 _atom_site_disorder_assembly
 _atom_site_disorder_group
Tl1 Tl 0.86360(18) 0.64536(19) 0.40728(8) 0.0379(4) Uani 1 1 d . . .
Tl2 Tl 0.49665(19) 0.6427(2) 0.23849(9) 0.0462(5) Uani 1 1 d . . .
Tl3 Tl 0.10798(18) 0.36735(19) 0.27427(8) 0.0368(4) Uani 1 1 d . . .
Tl4 Tl 0.1238(2) 0.3643(2) -0.07842(10) 0.0491(5) Uani 1 1 d . . .
Tl5 Tl 0.50259(18) 0.35940(19) 0.43829(8) 0.0377(4) Uani 1 1 d . . .
Ag1 Ag 0.4460(4) 0.0196(4) 0.4081(2) 0.0535(10) Uani 1 1 d . . .
Ag2 Ag 0.4806(4) 0.0479(5) 0.0697(2) 0.0772(14) Uani 1 1 d . . .
Ag3 Ag -0.4635(4) 0.0017(4) 0.2396(2) 0.0669(12) Uani 1 1 d . . .
Ag4 Ag 0.3783(4) 0.3523(5) 0.1620(2) 0.0685(12) Uani 1 1 d . . .
As1 As -0.0113(4) 0.8450(4) 0.22383(16) 0.0282(13) Uani 0.73(3) 1 d P . .
Sb1 Sb -0.0113(4) 0.8450(4) 0.22383(16) 0.0282(13) Uani 0.27(3) 1 d P . .
As2 As 0.2022(3) 0.8436(4) 0.04852(16) 0.0364(12) Uani 0.37(3) 1 d P . .
Sb2 Sb 0.2022(3) 0.8436(4) 0.04852(16) 0.0364(12) Uani 0.63(3) 1 d P . .
As3 As 0.0093(4) 0.1649(4) 0.44915(18) 0.0264(14) Uani 0.94(3) 1 d P . .
Sb3 Sb 0.0093(4) 0.1649(4) 0.44915(18) 0.0264(14) Uani 0.06(3) 1 d P . .
As4 As 0.1847(4) 0.8340(4) 0.38579(18) 0.0262(13) Uani 0.90(3) 1 d P . .
Sb4 Sb 0.1847(4) 0.8340(4) 0.38579(18) 0.0262(13) Uani 0.10(3) 1 d P . .
As5 As 0.1041(4) 0.1271(5) 0.1402(2) 0.0300(14) Uani 0.98(3) 1 d P . .
Sb5 Sb 0.1041(4) 0.1271(5) 0.1402(2) 0.0300(14) Uani 0.02(3) 1 d P . .
As6 As 0.6583(5) 0.3140(5) 0.0990(2) 0.0396(16) Uani 0.86(3) 1 d P . .
Sb6 Sb 0.6583(5) 0.3140(5) 0.0990(2) 0.0396(16) Uani 0.14(3) 1 d P . .
As7 As 0.7797(4) 0.1143(5) 0.31882(19) 0.0284(9) Uani 1 1 d . . .
S1 S 0.1883(10) 0.2685(12) 0.4275(5) 0.033(2) Uani 1 1 d . . .
S2 S 0.1742(11) 0.6708(12) 0.1533(5) 0.034(2) Uani 1 1 d . . .
```

```
S3 S 0.1756(11) 0.6589(11) 0.3212(5) 0.025(2) Uani 1 1 d . . .
S4 S -0.1994(11) 0.7412(12) 0.2416(5) 0.032(2) Uani 1 1 d . . .
S5 S 0.7412(11) 0.0032(11) 0.4223(5) 0.029(2) Uani 1 1 d . . .
S6 S -0.1698(11) 0.3145(11) 0.3503(5) 0.027(2) Uani 1 1 d . . .
S7 S 0.5070(11) 0.2586(11) 0.2823(5) 0.035(3) Uani 1 1 d . . .
S8 S 0.4627(11) 0.7549(12) 0.3953(5) 0.034(2) Uani 1 1 d . . .
S9 S 0.2046(12) 0.2917(13) 0.0887(5) 0.038(3) Uani 1 1 d . . .
S10 S -0.1704(10) 0.3335(10) 0.5161(4) 0.024(2) Uani 1 1 d . . .
S11 S -0.1487(11) 0.3120(11) 0.1734(5) 0.029(2) Uani 1 1 d . . .
S12 S 0.2451(11) 0.0191(12) 0.2418(5) 0.034(2) Uani 1 1 d . . .
S13 S 0.2498(12) 0.6106(12) 0.0014(5) 0.036(2) Uani 1 1 d . . .
S14 S 0.2451(12) 0.9518(13) -0.0968(6) 0.041(3) Uani 1 1 d . . .
S15 S 0.4810(11) 0.7818(13) 0.0764(5) 0.036(3) Uani 1 1 d . . .

loop_
 _atom_site_aniso_label
 _atom_site_aniso_U_11
 _atom_site_aniso_U_22
 _atom_site_aniso_U_33
 _atom_site_aniso_U_23
 _atom_site_aniso_U_13
 _atom_site_aniso_U_12
Tl1 0.0292(8) 0.0324(10) 0.0511(11) -0.0157(8) 0.0138(7) -0.0111(7)
Tl2 0.0315(9) 0.0493(12) 0.0614(12) -0.0268(9) 0.0187(8) -0.0168(8)
Tl3 0.0326(8) 0.0376(10) 0.0406(10) -0.0159(8) 0.0122(7) -0.0140(7)
Tl4 0.0313(9) 0.0479(11) 0.0645(13) -0.0168(9) 0.0110(8) -0.0134(8)
Tl5 0.0269(8) 0.0356(10) 0.0491(11) -0.0237(8) 0.0141(7) -0.0081(7)
Ag1 0.0289(16) 0.044(2) 0.093(3) -0.035(2) 0.0195(17) -0.0143(15)
Ag2 0.0328(19) 0.077(3) 0.139(4) -0.068(3) 0.032(2) -0.025(2)
Ag3 0.0244(17) 0.044(2) 0.129(4) -0.036(2) 0.006(2) -0.0072(16)
Ag4 0.045(2) 0.098(3) 0.070(3) -0.045(2) 0.0248(19) -0.029(2)
As1 0.0243(18) 0.037(2) 0.030(2) -0.0196(16) 0.0181(15) -0.0165(16)
Sb1 0.0243(18) 0.037(2) 0.030(2) -0.0196(16) 0.0181(15) -0.0165(16)
As2 0.0263(17) 0.041(2) 0.046(2) -0.0259(16) 0.0160(14) -0.0129(14)
Sb2 0.0263(17) 0.041(2) 0.046(2) -0.0259(16) 0.0160(14) -0.0129(14)
As3 0.0204(19) 0.032(2) 0.030(2) -0.0173(17) 0.0153(15) -0.0106(16)
Sb3 0.0204(19) 0.032(2) 0.030(2) -0.0173(17) 0.0153(15) -0.0106(16)
As4 0.0162(18) 0.031(2) 0.031(2) -0.0183(17) 0.0090(15) -0.0061(15)
Sb4 0.0162(18) 0.031(2) 0.031(2) -0.0183(17) 0.0090(15) -0.0061(15)
As5 0.027(2) 0.024(2) 0.042(3) -0.0191(19) 0.0169(17) -0.0106(17)
Sb5 0.027(2) 0.024(2) 0.042(3) -0.0191(19) 0.0169(17) -0.0106(17)
As6 0.032(2) 0.052(3) 0.038(3) -0.010(2) 0.0107(18) -0.023(2)
Sb6 0.032(2) 0.052(3) 0.038(3) -0.010(2) 0.0107(18) -0.023(2)
As7 0.0216(18) 0.028(2) 0.036(2) -0.0206(18) 0.0119(16) -0.0071(16)
S1 0.016(4) 0.036(6) 0.046(6) -0.015(5) 0.009(4) -0.009(4)
S2 0.026(5) 0.031(6) 0.043(6) -0.018(5) 0.021(4) -0.010(4)
S3 0.030(5) 0.015(5) 0.027(5) -0.009(4) 0.008(4) -0.006(4)
S4 0.035(5) 0.029(6) 0.044(6) -0.017(5) 0.016(5) -0.022(5)
S5 0.023(4) 0.024(5) 0.037(6) -0.012(4) 0.006(4) -0.006(4)
S6 0.034(5) 0.028(5) 0.029(5) -0.014(4) 0.014(4) -0.020(4)
S7 0.030(5) 0.017(5) 0.041(6) -0.007(4) 0.004(4) 0.005(4)
S8 0.022(5) 0.035(6) 0.047(6) -0.018(5) 0.015(4) -0.011(4)
S9 0.034(5) 0.044(7) 0.038(6) -0.014(5) 0.019(5) -0.018(5)
S10 0.027(4) 0.011(5) 0.029(5) -0.008(4) 0.015(4) -0.005(4)
S11 0.026(5) 0.025(5) 0.038(6) -0.021(5) 0.011(4) -0.008(4)
S12 0.030(5) 0.031(6) 0.037(6) -0.011(5) 0.012(4) -0.010(4)
S13 0.042(6) 0.031(6) 0.043(6) -0.018(5) 0.023(5) -0.021(5)
S14 0.031(5) 0.042(7) 0.053(7) -0.014(5) 0.003(5) -0.018(5)
S15 0.015(4) 0.050(7) 0.034(6) 0.003(5) 0.004(4) -0.013(4)

_geom_special_details
```

```
;
 All esds (except the esd in the dihedral angle between two l.s. planes)
 are estimated using the full covariance matrix.  The cell esds are taken
 into account individually in the estimation of esds in distances, angles
 and torsion angles; correlations between esds in cell parameters are only
 used when they are defined by crystal symmetry.  An approximate (isotropic)
 treatment of cell esds is used for estimating esds involving l.s. planes.
;

loop_
 _geom_bond_atom_site_label_1
 _geom_bond_atom_site_label_2
 _geom_bond_distance
 _geom_bond_site_symmetry_2
 _geom_bond_publ_flag
Tl1 S5 3.105(9) 1_565 ?
Tl2 Ag3 3.566(4) 1_665 ?
Tl3 S1 3.047(10) . ?
Tl3 S6 3.069(9) . ?
Tl3 S12 3.123(10) . ?
Tl3 Ag4 3.238(4) . ?
Tl4 S15 3.140(8) 2_665 ?
Tl5 S5 3.118(9) . ?
Ag1 S8 2.491(11) 1_545 ?
Ag1 S1 2.508(9) . ?
Ag1 S5 2.584(9) . ?
Ag2 S15 2.487(12) 1_545 ?
Ag2 S14 2.518(10) 2_665 ?
Ag2 S9 2.565(10) . ?
Ag2 Ag2 3.056(9) 2_655 ?
Ag2 Ag3 3.376(7) 1_655 ?
Ag3 S4 2.500(10) 1_545 ?
Ag3 S12 2.528(10) 1_455 ?
Ag3 S7 2.612(11) 1_455 ?
Ag3 Ag4 3.051(6) 1_455 ?
Ag3 Ag2 3.376(7) 1_455 ?
Ag3 Tl2 3.566(4) 1_445 ?
Ag4 S9 2.468(11) . ?
Ag4 S7 2.518(11) . ?
Ag4 As6 2.679(5) . ?
Ag4 S2 2.679(10) . ?
Ag4 Ag3 3.051(6) 1_655 ?
As1 S4 2.292(10) . ?
As1 S2 2.384(9) . ?
As1 S3 2.428(10) . ?
As2 S15 2.335(9) . ?
As2 S13 2.403(10) . ?
As2 S2 2.502(10) . ?
As3 S1 2.224(10) . ?
As3 S10 2.290(8) . ?
As3 S6 2.352(10) . ?
As4 S8 2.240(9) . ?
As4 S3 2.303(10) . ?
As4 S10 2.334(9) 2_566 ?
As5 S9 2.223(11) . ?
As5 S12 2.227(11) . ?
As5 S11 2.307(8) . ?
As6 S14 2.255(12) 2_665 ?
As6 S13 2.277(10) 2_665 ?
As6 S11 2.293(10) 1_655 ?
As7 S7 2.233(10) . ?
```

```
As7 S5 2.246(10) . ?
As7 S6 2.320(10) 1_655 ?
S4 Ag3 2.500(10) 1_565 ?
S5 Tl1 3.105(9) 1_545 ?
S6 As7 2.320(10) 1_455 ?
S7 Ag3 2.612(11) 1_655 ?
S8 Ag1 2.491(11) 1_565 ?
S10 Sb4 2.334(9) 2_566 ?
S10 As4 2.334(9) 2_566 ?
S11 Sb6 2.293(10) 1_455 ?
S11 As6 2.293(10) 1_455 ?
S12 Ag3 2.528(10) 1_655 ?
S13 Sb6 2.277(10) 2_665 ?
S13 As6 2.277(10) 2_665 ?
S14 Sb6 2.255(12) 2_665 ?
S14 As6 2.255(12) 2_665 ?
S14 Ag2 2.518(10) 2_665 ?
S15 Ag2 2.487(12) 1_565 ?
S15 Tl4 3.140(8) 2_665 ?

loop_
 _geom_angle_atom_site_label_1
 _geom_angle_atom_site_label_2
 _geom_angle_atom_site_label_3
 _geom_angle
 _geom_angle_site_symmetry_1
 _geom_angle_site_symmetry_3
 _geom_angle_publ_flag
S1 Tl3 S6 67.3(2) . . ?
S1 Tl3 S12 97.9(3) . . ?
S6 Tl3 S12 88.3(2) . . ?
S1 Tl3 Ag4 125.47(17) . . ?
S6 Tl3 Ag4 160.65(19) . . ?
S12 Tl3 Ag4 76.10(19) . . ?
S8 Ag1 S1 127.2(3) 1_545 . ?
S8 Ag1 S5 112.4(3) 1_545 . ?
S1 Ag1 S5 119.5(3) . . ?
S15 Ag2 S14 118.4(3) 1_545 2_665 ?
S15 Ag2 S9 118.2(3) 1_545 . ?
S14 Ag2 S9 117.9(4) 2_665 . ?
S15 Ag2 Ag2 68.9(3) 1_545 2_655 ?
S14 Ag2 Ag2 104.4(3) 2_665 2_655 ?
S9 Ag2 Ag2 118.0(3) . 2_655 ?
S15 Ag2 Ag3 93.8(3) 1_545 1_655 ?
S14 Ag2 Ag3 71.4(3) 2_665 1_655 ?
S9 Ag2 Ag3 81.4(3) . 1_655 ?
Ag2 Ag2 Ag3 158.2(2) 2_655 1_655 ?
S4 Ag3 S12 123.0(3) 1_545 1_455 ?
S4 Ag3 S7 127.1(3) 1_545 1_455 ?
S12 Ag3 S7 105.7(3) 1_455 1_455 ?
S4 Ag3 Ag4 138.5(3) 1_545 1_455 ?
S12 Ag3 Ag4 88.8(3) 1_455 1_455 ?
S7 Ag3 Ag4 52.1(2) 1_455 1_455 ?
S4 Ag3 Ag2 90.0(3) 1_545 1_455 ?
S12 Ag3 Ag2 85.0(3) 1_455 1_455 ?
S7 Ag3 Ag2 115.1(3) 1_455 1_455 ?
Ag4 Ag3 Ag2 64.80(13) 1_455 1_455 ?
S4 Ag3 Tl2 61.8(2) 1_545 1_445 ?
S12 Ag3 Tl2 61.2(2) 1_455 1_445 ?
S7 Ag3 Tl2 158.2(3) 1_455 1_445 ?
Ag4 Ag3 Tl2 137.77(15) 1_455 1_445 ?
```

Ag2 Ag3 Tl2 82.48(12) 1_455 1_445 ?
S9 Ag4 S7 138.0(4) . . ?
S9 Ag4 As6 107.7(3) . . ?
S7 Ag4 As6 97.9(3) . . ?
S9 Ag4 S2 98.8(4) . . ?
S7 Ag4 S2 103.8(3) . . ?
As6 Ag4 S2 108.7(3) . . ?
S9 Ag4 Ag3 89.9(3) . 1_655 ?
S7 Ag4 Ag3 54.9(2) . 1_655 ?
As6 Ag4 Ag3 94.05(16) . 1_655 ?
S2 Ag4 Ag3 151.6(3) . 1_655 ?
S9 Ag4 Tl3 85.7(2) . . ?
S7 Ag4 Tl3 66.7(2) . . ?
As6 Ag4 Tl3 164.56(18) . . ?
S2 Ag4 Tl3 75.8(2) . . ?
Ag3 Ag4 Tl3 77.90(13) 1_655 . ?
S4 As1 S2 100.0(3) . . ?
S4 As1 S3 93.0(4) . . ?
S2 As1 S3 88.2(3) . . ?
S15 As2 S13 100.0(4) . . ?
S15 As2 S2 95.5(3) . . ?
S13 As2 S2 81.5(3) . . ?
S1 As3 S10 101.0(3) . . ?
S1 As3 S6 95.5(4) . . ?
S10 As3 S6 92.8(3) . . ?
S8 As4 S3 101.3(3) . . ?
S8 As4 S10 98.1(4) . 2_566 ?
S3 As4 S10 89.9(3) . 2_566 ?
S9 As5 S12 105.4(4) . . ?
S9 As5 S11 100.9(4) . . ?
S12 As5 S11 98.4(3) . . ?
S14 As6 S13 98.8(4) 2_665 2_665 ?
S14 As6 S11 103.0(4) 2_665 1_655 ?
S13 As6 S11 99.9(4) 2_665 1_655 ?
S14 As6 Ag4 96.1(3) 2_665 . ?
S13 As6 Ag4 142.9(3) 2_665 . ?
S11 As6 Ag4 109.5(3) 1_655 . ?
S7 As7 S5 97.0(4) . . ?
S7 As7 S6 100.5(4) . 1_655 ?
S5 As7 S6 98.1(4) . 1_655 ?
As3 S1 Ag1 99.7(4) . . ?
As3 S1 Tl3 96.4(3) . . ?
Ag1 S1 Tl3 88.4(3) . . ?
As1 S2 As2 108.4(4) . . ?
As1 S2 Ag4 137.6(4) . . ?
As2 S2 Ag4 113.6(3) . . ?
As4 S3 As1 102.2(3) . . ?
As1 S4 Ag3 98.5(4) . 1_565 ?
As7 S5 Ag1 103.9(4) . . ?
As7 S5 Tl1 101.5(3) . 1_545 ?
Ag1 S5 Tl1 82.8(3) . 1_545 ?
As7 S5 Tl5 85.7(3) . . ?
Ag1 S5 Tl5 78.1(2) . . ?
Tl1 S5 Tl5 160.7(3) 1_545 . ?
As7 S6 As3 100.0(4) 1_455 . ?
As7 S6 Tl3 114.0(3) 1_455 . ?
As3 S6 Tl3 93.1(3) . . ?
As7 S7 Ag4 128.4(4) . . ?
As7 S7 Ag3 87.1(3) . 1_655 ?
Ag4 S7 Ag3 73.0(3) . 1_655 ?
As4 S8 Ag1 97.9(3) . 1_565 ?

```
As5 S9 Ag4 115.9(4) . . ?
As5 S9 Ag2 91.0(4) . . ?
Ag4 S9 Ag2 86.7(3) . . ?
As3 S10 Sb4 106.5(3) . 2_566 ?
As3 S10 As4 106.5(3) . 2_566 ?
Sb4 S10 As4 0.00(18) 2_566 2_566 ?
Sb6 S11 As6 0.0(2) 1_455 1_455 ?
Sb6 S11 As5 102.1(3) 1_455 . ?
As6 S11 As5 102.1(3) 1_455 . ?
As5 S12 Ag3 111.8(4) . 1_655 ?
As5 S12 Tl3 89.7(3) . . ?
Ag3 S12 Tl3 88.2(3) 1_655 . ?
Sb6 S13 As6 0.0(3) 2_665 2_665 ?
Sb6 S13 As2 96.8(4) 2_665 . ?
As6 S13 As2 96.8(4) 2_665 . ?
Sb6 S14 As6 0.0(3) 2_665 2_665 ?
Sb6 S14 Ag2 99.8(4) 2_665 2_665 ?
As6 S14 Ag2 99.8(4) 2_665 2_665 ?
As2 S15 Ag2 105.7(4) . 1_565 ?
As2 S15 Tl4 162.2(5) . 2_665 ?
Ag2 S15 Tl4 85.4(3) 1_565 2_665 ?

_diffrn_measured_fraction_theta_max    0.994
_diffrn_reflns_theta_full              29.83
_diffrn_measured_fraction_theta_full   0.965
_refine_diff_density_max    3.053
_refine_diff_density_min   -7.780
_refine_diff_density_rms    0.718
```